

Importance of Platinum(II)-Assisted Platinum(IV) Substitution for the Oxidation of Guanosine Derivatives by Platinum(IV) Complexes

Sunhee Choi,^{*,†} Livia Vastag,[†] Yuri C. Larrabee,[†] Michelle L. Personick,[†] Kurt B. Schaberg,[†] Benjamin J. Fowler,[†] Roger K. Sandwick,[†] and Gulnar Rawji[‡]

Department of Chemistry and Biochemistry, Middlebury College, Middlebury, Vermont 05753, and Department of Chemistry, Southwestern University, Georgetown, Texas 78626

Received September 20, 2007

Guanosine derivatives with a nucleophilic group at the 5' position (G-5') are oxidized by the Pt^{IV} complex Pt(*d,l*)(1,2-(NH₂)₂C₆H₁₀)Cl₄ ([Pt^{IV}(dach)Cl₄]). The overall redox reaction is autocatalytic, consisting of the Pt^{II}-catalyzed Pt^{IV} substitution and two-electron transfer between Pt^{IV} and the bound G-5'. In this paper, we extend the study to improve understanding of the redox reaction, particularly the substitution step. The [Pt^{II}(NH₃)₂(CBDCA-O,O')] (CBDCA = cyclobutane-1,1-dicarboxylate) complex effectively accelerates the reactions of [Pt^{IV}(dach)Cl₄] with 5'-dGMP and with cGMP, indicating that the Pt^{II} complex does not need to be a Pt^{IV} analogue to accelerate the substitution. Liquid chromatography/mass spectroscopy (LC/MS) analysis showed that the [Pt^{IV}(dach)Cl₄]/[Pt^{II}(NH₃)₂(CBDCA-O,O')]/cGMP reaction mixture contained two Pt^{IV}cGMP adducts, [Pt^{IV}(NH₃)₂(cGMP)(Cl)(CBDCA-O,O')] and [Pt^{IV}(dach)(cGMP)Cl₃]. The LC/MS studies also indicated that the *trans,cis*-[Pt^{IV}(dach)(³⁷Cl)(³⁵Cl)₂]/[Pt^{II}(en)(³⁵Cl)₂]/9-EtG mixture contained two Pt^{IV}-9-EtG adducts, [Pt^{IV}(en)(9-EtG)(³⁷Cl)(³⁵Cl)₂] and [Pt^{IV}(dach)(9-EtG)(³⁷Cl)(³⁵Cl)₂]. These Pt^{IV}G products are predicted by the Basolo–Pearson (BP) Pt^{II}-catalyzed Pt^{IV}-substitution scheme. The substitution can be envisioned as an oxidative addition reaction of the planar Pt^{II} complex where the entering ligand G and the chloro ligand from the axial position of the Pt^{IV} complex are added to Pt^{II} in the axial positions. From the point of view of reactant Pt^{IV}, an axial chloro ligand is thought to be substituted by the entering ligand G. The Pt^{IV} complexes without halo axial ligands such as *trans,cis*-[Pt(en)(OH)₂Cl₂], *trans,cis*-[Pt(en)(OCOCF₃)₂Cl₂], and *cis,trans,cis*-[Pt(NH₃)(C₆H₁₁NH₂)(OCOCH₃)₂Cl₂] ([Pt^{IV}(a,cha)(OCOCH₃)₂Cl₂], satraplatin) did not react with 5'-dGMP. The bromo complex, [Pt^{IV}(en)Br₄], showed a significantly faster substitution rate than the chloro complexes, [Pt^{IV}(en)Cl₄] and [Pt^{IV}(dach)Cl₄]. The results indicate that the axial halo ligands are essential for substitution and the Pt^{IV} complexes with larger axial halo ligands have faster rates. When the Pt^{IV} complexes with different carrier ligands were compared, the substitution rates increased in the order [Pt^{IV}(dach)Cl₄] < [Pt^{IV}(en)Cl₄] < [Pt^{IV}(NH₃)₂Cl₄], which is in reverse order to the carrier ligand size. These axial and carrier ligand effects on the substitution rates are consistent with the BP mechanism. Larger axial halo ligands can form a better bridging ligand, which facilitates the electron-transfer process from the Pt^{II} to Pt^{IV} center. Smaller carrier ligands exert less steric hindrance for the bridge formation.

Introduction

Platinum coordination complexes are biologically important for their anticancer activity, being effective on tumor types including testicular, ovarian, and colon cancers.¹ The three platinum anticancer drugs currently available on the

market, cisplatin, carboplatin, and oxaliplatin, all have an oxidation state of 2+. Because of severe side effects and other deficiencies, however, alternative platinum anticancer drugs are under development. A wide variety Pt^{IV} complexes have potential as powerful anticancer drugs, and they can be administered orally.² A prototypical member of this class, *cis,trans,cis*-[Pt(NH₃)(C₆H₁₁NH₂)(OC(O)CH₃)₂Cl₂] (satrapl-

* To whom correspondence should be addressed. E-mail: choi@middlebury.edu.

[†] Middlebury College.

[‡] Southwestern University.

(1) (a) Fuertes, M. A.; Alonso, C.; Perez, J. M. *Chem. Rev.* **2003**, *103*, 645–662. (b) Lippert, B. *Cisplatin: Chemistry and Biochemistry of a Leading Anticancer Drug*; Wiley-VCH: Weinheim, Germany, 1999.

atin), is currently undergoing phase III clinical trials. Because Pt^{IV} complexes are kinetically inert,³ it is generally believed they must be reduced to their Pt^{II} analogues in vivo to bind to DNA and achieve anticancer activity.² However, while direct Pt^{IV} binding to DNA has been observed in vitro in several laboratories,^{4,5} a detailed mechanism was not proposed.

Our laboratory reported that Pt^{IV} complexes have a wide range of reactivity depending on their structures.⁶ For example, [Pt^{IV}(dach)Cl₄] was reduced by ascorbic acid approximately 700 times faster than *cis,trans,cis*-[Pt((CH₃)₂-CHNH₂)₂(OH)₂Cl₂], while *trans,cis*-[Pt^{IV}(en)(OH)₂Cl₂] resisted reduction completely. The [Pt^{IV}(dach)Cl₄] complex reacted with 5'-GMP approximately 5 times faster than [Pt^{IV}(en)Cl₄], which, in turn, was 10-fold faster than *trans,cis*-[Pt^{IV}(en)-(OCOCH₃)₂Cl₂]. The *trans,cis*-[Pt^{IV}(en)(OH)₂Cl₂] complex did not significantly react with 5'-GMP.⁷

The most reactive complex, [Pt^{IV}(dach)Cl₄], oxidized 5'-dGMP,⁸ 3'-dGMP,⁹ and 5'-d[GTTTT]-3'.⁹ The redox mechanism consists of two steps: a substitution and an electron transfer.^{8,9} In the substitution reaction, Pt^{IV} binds to the N7 of the guanosine (G) moiety. In the electron-transfer reaction, the 5'-phosphate or 5'-hydroxyl group attacks C8 of the G moiety and an inner-sphere, two-electron transfer produces cyclic (5'-O-C8)-G and a Pt^{II} complex. The identity of the final oxidized G depends on the hydrolysis rate of the cyclic intermediate. The cyclic phosphodiester intermediate formed from [Pt^{IV}(dach)Cl₄]/5'-dGMP is hydrolyzed to 8-oxo-5'-dGMP.⁸ However, the cyclic ether intermediate formed from [Pt^{IV}(dach)Cl₄]/3'-dGMP (or 5'-d[GTTTT]) does not hydrolyze, and this cyclic form is the final oxidation product.⁹ The lack of a 5'-nucleophilic group in the G moiety, such as in 3',5'-cyclic guanosine monophosphate (cGMP), 9-me-

thylxanthine (9-Mxan), 5'-d[TTGTT]-3', and 5'-d[TTTTG]-3', prevents the electron-transfer step, and only the substitution step is observed.⁹

The kinetics of the redox reactions between [Pt^{IV}(dach)Cl₄] and 5'- (and 3'-)dGMP is autocatalytic.¹⁰ Catalyzed by Pt^{II} complexes, the reaction seems to follow the classic Basolo–Pearson (BP) Pt^{II}-catalyzed Pt^{IV} substitution.^{10,11} However, several important questions remain unanswered to confirm this mechanism. First, our previous study showed that the Pt^{II} complexes do not have to be their Pt^{IV} analogues to accelerate the reaction. Furthermore, all of the Pt^{II} complexes studied previously contained at least one leaving chloro ligand.¹⁰ Can Pt^{II} without a leaving halo group accelerate the reaction? Second, the previous studies showed that a chloro ligand in [Pt^{IV}(dach)Cl₄] is substituted by G.^{8,10} Which chloro ligand, axial or equatorial, is substituted? Third, in the previous studies we used only two Pt^{IV} complexes, namely, [Pt^{IV}(dach)Cl₄] and [Pt^{IV}(en)Cl₄].¹⁰ Does the BP mechanism apply to other Pt^{IV} complexes? What are the effects of the Pt^{IV} axial and carrier ligands? These questions are addressed by using several Pt^{IV} complexes with different axial and carrier ligands (Chart 1).

Experimental Section

Sample Preparation. [Pt^{IV}(dach)Cl₄] and [Pt^{II}(NH₃)₂(CBDCA-O,O')] were obtained from the National Cancer Institute, Drug Synthesis and Chemistry Branch, Developmental Therapeutics Program, Division of Cancer Treatment. Satraplatin was obtained through a material transfer agreement with GPC Biotech AG. Isotopically pure Na³⁵Cl and Na³⁷Cl were obtained from Oak Ridge National Laboratory, Oak Ridge, TN. The complexes [Pt^{II}(en)Cl₂], [Pt^{IV}(en)Cl₄], [Pt^{IV}(en)Br₄], *trans,cis*-[Pt^{IV}(en)(OCOFC₃)₂Cl₂], *trans,cis*-[Pt^{IV}(en)(OH)₂Cl₂], *cis*-[Pt^{IV}(NH₃)₂Cl₄], and *trans*-(*R,R*)-[Pt^{II}(dach)I₂] were synthesized following previously published procedures.¹²

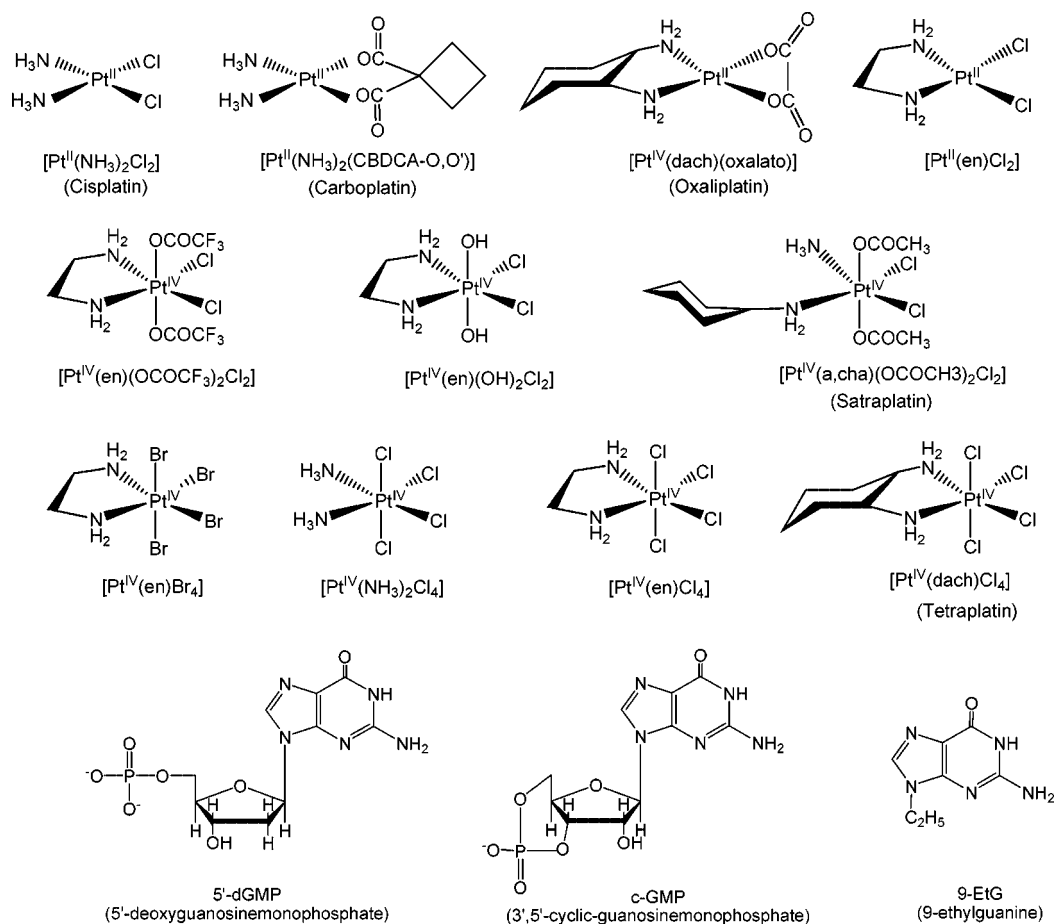
trans-(*R,R*)-[Pt^{II}(dach)³⁵(Cl)₂] was prepared from the corresponding diiodo complex according to a literature procedure with minor modifications.¹² *trans*-(*R,R*)-Diaminocyclohexanediiodoplatinum(II) (0.024 mmol) was suspended in 0.5 mL each of water and acetone. Solid AgNO₃ was added, and the resulting milky suspension stirred at room temperature in the dark until no more *trans*-(*R,R*)-[Pt^{II}(dach)I₂] remained (~2 h). Silver iodide was removed by filtration through Celite packed in a pasteur pipet. A 10-fold excess of Na³⁵Cl (0.24 mmol) was added to the filtrate and the solution stirred at 50 °C for about 2 h. A pale-yellow solid that precipitated was collected, washed with water and acetone, and dried under vacuum. Yield: ~78%. LC/MS: *m/z* 324.9.

trans-(*R,R*)-*cis,trans*-[Pt^{IV}(dach)³⁵(Cl)₂(³⁷Cl)₂] was prepared by adapting literature procedures.¹² Hydrogen peroxide (0.20 mmol) was added to a suspension of *trans*-(*R,R*)-[Pt^{II}(dach)³⁵Cl₂] (0.016 mmol) in 0.5 mL of water. The mixture was stirred at 70 °C for 2 h, during which *trans*-(*R,R*)-[Pt^{IV}(dach)³⁵Cl₂(OH)₂], a lighter-

- (2) (a) Hall, M. D.; Hambley, T. W. *Coord. Chem. Rev.* **2002**, *232*, 49–67. (b) Eastman, A. *Biochem. Pharmacol.* **1987**, *36*, 4177–4178. (c) Chaney, S. G. *Int. J. Oncol.* **1995**, *6*, 1291–1305. (d) Chaney, S. G.; Gibbons, G. R.; Wyrick, S. D.; Podhasky, P. *Cancer Res.* **1991**, *51*, 969–973. (e) Kelland, L. R.; Murrer, B. A.; Abel, G.; Giandomenico, C. M.; Mistry, P.; Harrap, K. R. *Cancer Res.* **1992**, *52*, 822–828. (f) Oshita, F.; Eastman, A. *Oncol. Res.* **1993**, *5*, 111–118. (g) Yoshida, M.; Khokhar, A. R.; Zhang, Y.-P.; Siddik, Z. H. *Cancer Res.* **1994**, *54*, 4691–4697.
- (3) (a) Hartley, F. R. *Chemistry of the Platinum Group Metals: Recent Developments*; Elsevier: Amsterdam, 1991. (b) Basolo, F.; Pearson, R. G. *Mechanism of Inorganic Reactions*; Wiley: New York, 1967.
- (4) (a) Novakova, O.; Vrana, O.; Kiseleva, V. I.; Brabec, V. *Eur. J. Biochem.* **1995**, *228*, 616–624. (b) Talman, E. G.; Kidani, Y.; Mohrmann, L.; Reedijk, J. *Inorg. Chim. Acta* **1998**, *283*, 251–255. (c) Galanski, M.; Keppler, B. K. *Inorg. Chim. Acta* **2000**, *300*–302, 783–789.
- (5) (a) Roat, R. M.; Reedijk, J. *J. Inorg. Biochem.* **1993**, *52*, 263–274. (b) Talman, E. G.; Brüning, W.; Reedijk, J.; Spek, A. L.; Veldman, N. *Inorg. Chem.* **1997**, *36*, 854–861. (c) van der Veer, J. L.; Peters, A. R.; Reedijk, J. *J. Inorg. Biochem.* **1986**, *26*, 137–142. (d) Roat, R. M.; Jerardi, M. J.; Kopay, C. B.; Heath, D. C.; Clark, J. A.; DeMars, J. A.; Weaver, J. M.; Bezemer, E.; Reedijk, J. *J. Chem. Soc., Dalton Trans.* **1997**, 3615–3621.
- (6) Choi, S.; Filotto, C.; Bisanzo, M.; Delaney, S.; Lagasee, D.; Whitworth, J. L.; Jusko, A.; Li, C.; Wood, N. A.; Willingham, J.; Schwenker, A.; Spaulding, K. *Inorg. Chem.* **1998**, *37*, 2500–2504.
- (7) Choi, S.; Mahalingaiah, S.; Delaney, S.; Neale, N. R.; Masood, S. *Inorg. Chem.* **1999**, *38*, 1800–1805.
- (8) Choi, S.; Cooley, R. B.; Hakemian, A. S.; Larrabee, Y. C.; Bunt, R. C.; Maupaus, S. D.; Muller, J. G.; Burrows, C. J. *J. Am. Chem. Soc.* **2004**, *126*, 591–598.
- (9) Choi, S.; Cooley, R. B.; Voutchkova, A.; Leung, C. H.; Vastag, L.; Knowles, D. E. *J. Am. Chem. Soc.* **2005**, *127*, 1773–1781.

- (10) Choi, S.; Vastag, L.; Leung, C. H.; Beard, A. M.; Knowles, D. E.; Larrabee, J. A. *Inorg. Chem.* **2006**, *45*, 10108–10114.
- (11) (a) Basolo, F.; Wilks, P. H.; Pearson, R. G.; Wilkins, R. G. *J. Inorg. Nucl. Chem.* **1958**, *6*, 161. (b) Mason, W. R. **1972**, *7*, 241–255. (c) Summa, G. M.; Scott, B. A. *Inorg. Chem.* **1980**, *19*, 1079. (d) Cox, L. T.; Collins, S. B.; Martin, D. S. *J. Inorg. Nucl. Chem.* **1961**, *17*, 383.
- (12) (a) Ellis, L. T.; Er, H. M.; Hambley, T. W. *Aust. J. Chem.* **1995**, *48*, 793–806. (b) Al-Baker, S.; Siddik, Z. H.; Khokhar, A. R. *J. Coord. Chem.* **1994**, *31*, 109–116.

Chart 1. Structures of the Platinum Complexes and Guanine Derivatives Studied



yellow solid, was formed. The dihydroxo complex generated in situ was converted to the tetrachloro complex by the addition of excess $Na^{37}Cl$ (0.23 mmol) and HNO_3 (0.04 mmol), followed by stirring at 70 °C for an additional 2 h. The suspended solid changed from a yellow to an orange, which redissolved upon the addition of acetone (0.5 mL) and further stirring for another 30 min. The resulting pale-yellow solution was filtered and the filtrate evaporated to dryness, leaving a residue of excess $Na^{37}Cl$ and the desired product as a yellow solid. The product complex was obtained by the addition of acetone to the residue and removal of the undissolved solid ($Na^{37}Cl$) by filtration. Evaporation of acetone yielded the final product as yellow crystals. Yield: ~93%. LC/MS: m/z 454.9.

In every step of the synthesis, amber glassware or glassware wrapped in aluminum foil was used to avoid photoreduction of the platinum complexes. The products were characterized by IR (Bruker Equinox 55 spectrometer), 1H NMR (Bruker 400 Ultrashield spectrometer), high-performance liquid chromatography (HPLC; Waters Alliance 2695 equipped with a Waters 2996 photodiode array detector and a Waters Atlantis dC18 column), and liquid chromatography/mass spectrometry (LC/MS). Stock platinum complex solutions were prepared by dissolution in saline water (0.1 M NaCl, pH 8.3–8.6). The pH was adjusted to 8.3–8.6 to fully deprotonate the phosphate group in 5'-dGMP.¹⁰ To prevent hydrolysis of the platinum complexes, 0.1 M NaCl and 0.1 M KBr solutions were used for the chloro and bromo complexes, respectively.

Mass Spectrometry. LC/MS analyses were conducted on an 1100 series LC and LC/MSD Trap XCT Plus from Agilent Technologies. The LC component was equipped with a photodiode array detector and an Eclipse X-D8-C8 column (5 μm , 4.6 \times 150

mm), run under isocratic (0.5 mL min^{-1}) conditions with a solvent of 0.5% formic acid in water. An ion-trap mass spectrometer to select for specific masses was used with fragmentation both on and off. The MS parameters were set to scan from m/z 50 to 2200 using positive or negative detection with electrospray ionization mass spectrometry. For tuning, the nebulizer was set to 50 psi, the dry gas flow to 9 L min^{-1} , and the dry temperature to 365 °C.

Kinetic Studies. An appropriate amount of 5'-dGMP was added to vials containing equal volumes of platinum stock and saline solutions. The pH values of the solutions were adjusted to pH 8.3 with NaOH using a pH meter (Orion Research 960) equipped with a Mettler-Toledo Inlab combination pH microelectrode. Attainment of the desired pH constituted the beginning of the reaction. UV/vis spectra were obtained in 10-mm cells on a Varian Cary 4000i spectrophotometer with Cary WinUV kinetic assay software. The absorbances at 360 and 390 nm were monitored. The sample temperature was maintained by a Varian-Cary temperature controller. Kinetic experiments were repeated at least three times.

Results

Synthesis of Pt^{II} and Pt^{IV} Complexes with Isotopically Pure ^{35}Cl and ^{37}Cl . The key complexes $[Pt^{II}(en)(^{35}Cl)_2]$, *trans*-(*R,R*)- $[Pt^{II}(dach)(^{35}Cl)_2]$, and *trans*-(*R,R*)-*cis,trans*- $[Pt^{IV}(dach)(^{35}Cl)_2(^{37}Cl)_2]$ were synthesized by modification of published procedures¹² and characterized by LC/MS.

In the reactions of the diiodo complexes with $AgNO_3$, the addition of acetone facilitated better mixing of the suspension and reduced reaction times for complete precipitation of AgI , particularly for the complex with *dach* as the diamine. The

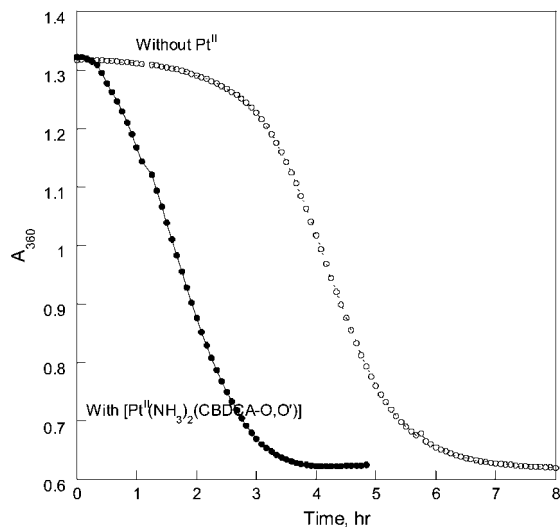


Figure 1. Absorbance at 360 nm vs time of the reactions of 5 mM $[\text{Pt}^{\text{IV}}(\text{dach})\text{Cl}_4]$ and 20 mM 5'-dGMP with and without 1 mM $[\text{Pt}^{\text{II}}(\text{NH}_3)_2(\text{CBDCA-O,O}')]$ in 100 mM NaCl, pH 8.2 at 40 °C. The absorbance at 360 nm is due to $[\text{Pt}^{\text{IV}}(\text{dach})\text{Cl}_4]$, $[\text{Pt}^{\text{IV}}(\text{dach})(5'\text{-dGMP})\text{Cl}_3]$, and $[\text{Pt}^{\text{IV}}(\text{NH}_3)_2(5'\text{-dGMP})\text{Cl}(\text{CBDCA-O,O}')]$.

target complex $[\text{Pt}^{\text{IV}}(\text{dach})(^{35}\text{Cl})_2(^{37}\text{Cl})_2]$ obtained from the reaction of $[\text{Pt}^{\text{IV}}(\text{dach})(\text{OH})_2\text{Cl}_2]$ was generated in situ with Cl^- ions under acidic conditions. This step is usually accomplished by using HCl as both the source of the acid as well as the chloride. For this synthesis, however, NaCl and HNO_3 were used instead because Na^{37}Cl was the only available source for $^{37}\text{Cl}^-$. A larger excess of Na^{37}Cl relative to the acid was used to ensure a reasonable yield.

Reactions of $[\text{Pt}^{\text{IV}}(\text{dach})\text{Cl}_4]$ and 5'-dGMP with and without $[\text{Pt}^{\text{II}}(\text{NH}_3)_2(\text{CBDCA-O,O}')]$. Figure 1 compares the time course of A_{360} of the $[\text{Pt}^{\text{IV}}(\text{dach})\text{Cl}_4]$ and 5'-dGMP reaction with and without $[\text{Pt}^{\text{II}}(\text{NH}_3)_2(\text{CBDCA-O,O}')]$. Without $[\text{Pt}^{\text{II}}(\text{NH}_3)_2(\text{CBDCA-O,O}')]$, there is a long induction time for the reaction to start, which is significantly shortened by the addition of $[\text{Pt}^{\text{II}}(\text{NH}_3)_2(\text{CBDCA-O,O}')]$. This clearly indicates that $[\text{Pt}^{\text{II}}(\text{NH}_3)_2(\text{CBDCA-O,O}')]$ accelerates the redox reaction between $[\text{Pt}^{\text{IV}}(\text{dach})\text{Cl}_4]$ and 5'-dGMP.

Reactions of $[\text{Pt}^{\text{IV}}(\text{dach})\text{Cl}_4]$ and cGMP with and without $[\text{Pt}^{\text{II}}(\text{NH}_3)_2(\text{CBDCA-O,O}')]$. Figure 2 compares the time course of A_{360} and A_{390} of the $[\text{Pt}^{\text{IV}}(\text{dach})\text{Cl}_4]$ and cGMP reaction with and without $[\text{Pt}^{\text{II}}(\text{NH}_3)_2(\text{CBDCA-O,O}')]$. For both reactions, A_{360} does not change while A_{390} increases to a maximum without decreasing. A_{360} is mainly due to the Pt^{IV} complexes and is an excellent indication of the redox reaction because Pt^{II} complexes do not absorb at 360 nm. A_{390} is primarily due to the Pt^{IV} cGMP adducts. Absorbance at 390 nm without $[\text{Pt}^{\text{II}}(\text{NH}_3)_2(\text{CBDCA-O,O}')]$ is due to only $[\text{Pt}^{\text{IV}}(\text{dach})(\text{cGMP})\text{Cl}(\text{CBDCA-O,O}')]$. Absorbance at 390 nm with $[\text{Pt}^{\text{II}}(\text{NH}_3)_2(\text{CBDCA-O,O}')]$ is due to both $[\text{Pt}^{\text{IV}}(\text{NH}_3)_2(\text{cGMP})\text{Cl}(\text{CBDCA-O,O}')]$ and $[\text{Pt}^{\text{IV}}(\text{dach})(\text{cGMP})\text{Cl}(\text{CBDCA-O,O}')]$. The molar absorptivity of $[\text{Pt}^{\text{IV}}(\text{NH}_3)_2(\text{cGMP})\text{Cl}(\text{CBDCA-O,O}')]$ is approximately twice as big as that of $[\text{Pt}^{\text{IV}}(\text{dach})(\text{cGMP})\text{Cl}(\text{CBDCA-O,O}')]$, which is the reason why the final A_{390} with $[\text{Pt}^{\text{II}}(\text{NH}_3)_2(\text{CBDCA-O,O}')]$ is higher than that without it. A_{390} only due to $[\text{Pt}^{\text{IV}}(\text{dach})(\text{cGMP})\text{Cl}(\text{CBDCA-O,O}')]$ in the presence of the $[\text{Pt}^{\text{II}}(\text{NH}_3)_2(\text{CBDCA-O,O}')]$ reaction was calculated from the molar absorptivity

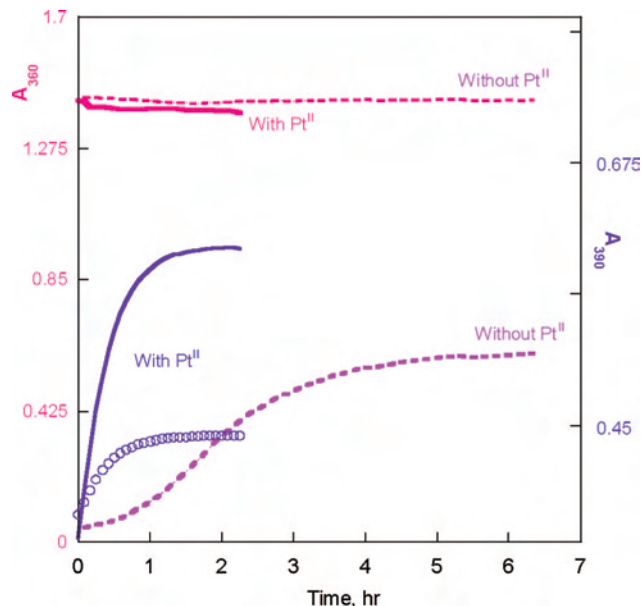


Figure 2. A_{360} and A_{390} vs time of the reactions of 5 mM $[\text{Pt}^{\text{IV}}(\text{dach})\text{Cl}_4]$ and 20 mM cGMP with and without 2 mM $[\text{Pt}^{\text{II}}(\text{NH}_3)_2(\text{CBDCA-O,O}')]$ in 100 mM NaCl at 50 °C and pH 8.2. A_{360} and A_{390} are shown in pink and purple, respectively. The open circle is the calculated A_{390} only due to $[\text{Pt}^{\text{IV}}(\text{dach})(\text{cGMP})\text{Cl}(\text{CBDCA-O,O}')]$.

ratios of $[\text{Pt}^{\text{IV}}(\text{dach})(\text{cGMP})\text{Cl}(\text{CBDCA-O,O}')]$ and $[\text{Pt}^{\text{IV}}(\text{NH}_3)_2(\text{cGMP})\text{Cl}(\text{CBDCA-O,O}')]$ and plotted in Figure 2 marked as open circles. The maximum 3 mM of $[\text{Pt}^{\text{IV}}(\text{dach})(\text{cGMP})\text{Cl}(\text{CBDCA-O,O}')]$ from 5 mM $[\text{Pt}^{\text{IV}}(\text{dach})\text{Cl}_4]$ and 2 mM $[\text{Pt}^{\text{II}}(\text{NH}_3)_2(\text{CBDCA-O,O}')]$ was generated after 1 h. The same concentration of $[\text{Pt}^{\text{IV}}(\text{dach})(\text{cGMP})\text{Cl}(\text{CBDCA-O,O}')]$ was generated after 2 h from the 5 mM $[\text{Pt}^{\text{IV}}(\text{dach})\text{Cl}_4]$ solution without $[\text{Pt}^{\text{II}}(\text{NH}_3)_2(\text{CBDCA-O,O}')]$. The results indicate that cGMP simply binds to $[\text{Pt}^{\text{IV}}(\text{dach})\text{Cl}_4]$ without a redox reaction. The addition of $[\text{Pt}^{\text{II}}(\text{NH}_3)_2(\text{CBDCA-O,O}')]$ expedites the binding, indicating that $[\text{Pt}^{\text{II}}(\text{NH}_3)_2(\text{CBDCA-O,O}')]$ accelerates the chloride substitution of $[\text{Pt}^{\text{IV}}(\text{dach})\text{Cl}_4]$ by cGMP.

The products of the $[\text{Pt}^{\text{IV}}(\text{dach})\text{Cl}_4]/[\text{Pt}^{\text{II}}(\text{NH}_3)_2(\text{CBDCA-O,O}')]/\text{cGMP}$ mixture were identified by LC/MS (Figure 3). The peaks at m/z 749.9 and 757.9 correspond to $[\text{Pt}^{\text{IV}}(\text{NH}_3)_2(\text{cGMP})\text{Cl}(\text{CBDCA-O,O}')]$ and $[\text{Pt}^{\text{IV}}(\text{dach})(\text{cGMP})\text{Cl}_3]$, respectively.

Reaction of *trans,cis*- $[\text{Pt}^{\text{IV}}(\text{dach})(^{37}\text{Cl})_2(^{35}\text{Cl})_2]$, $[\text{Pt}^{\text{II}}(\text{en})(^{35}\text{Cl})_2]$, and 9-EtG. Figure 4 displays the LC/MS spectra of the *trans,cis*- $[\text{Pt}^{\text{IV}}(\text{dach})(^{37}\text{Cl})_2(^{35}\text{Cl})_2]/[\text{Pt}^{\text{II}}(\text{en})(^{35}\text{Cl})_2]/9\text{-EtG}$ reaction mixture. The reactants $[\text{Pt}^{\text{II}}(\text{en})(^{35}\text{Cl})_2]$, *trans,cis*- $[\text{Pt}^{\text{IV}}(\text{dach})(^{37}\text{Cl})_2(^{35}\text{Cl})_2]$, and 9-EtG are detected at m/z 324.9, 454.9, and 177.9, respectively. Two main products are found at m/z 539.9 and 596.0. The 539.9 amu is equivalent to the mass of $[\text{Pt}^{\text{IV}}(\text{en})(9\text{-EtG})(^{37}\text{Cl})(^{35}\text{Cl})_2]$, which is the sum of 324.9 ($[\text{Pt}^{\text{II}}(\text{en})(^{35}\text{Cl})_2]$), 36.97 (^{37}Cl), and 177.9 (9-EtG) amu. This means ^{37}Cl and 9-EtG are added to the axial position of $[\text{Pt}^{\text{II}}(\text{en})(^{35}\text{Cl})_2]$, producing *trans,cis*- $[\text{Pt}^{\text{IV}}(\text{en})(9\text{-EtG})(^{37}\text{Cl})(^{35}\text{Cl})_2]$. The 596.0 amu is equivalent to the mass of $[\text{Pt}^{\text{IV}}(\text{dach})(9\text{-EtG})(^{37}\text{Cl})(^{35}\text{Cl})_2]$, which is the subtraction of 36.97 amu (^{37}Cl) from 454.9 amu ($[\text{Pt}^{\text{IV}}(\text{dach})(^{37}\text{Cl})_2(^{35}\text{Cl})_2]$) and the addition of 177.9 amu (9-EtG). This is a result of axial ^{37}Cl breaking from

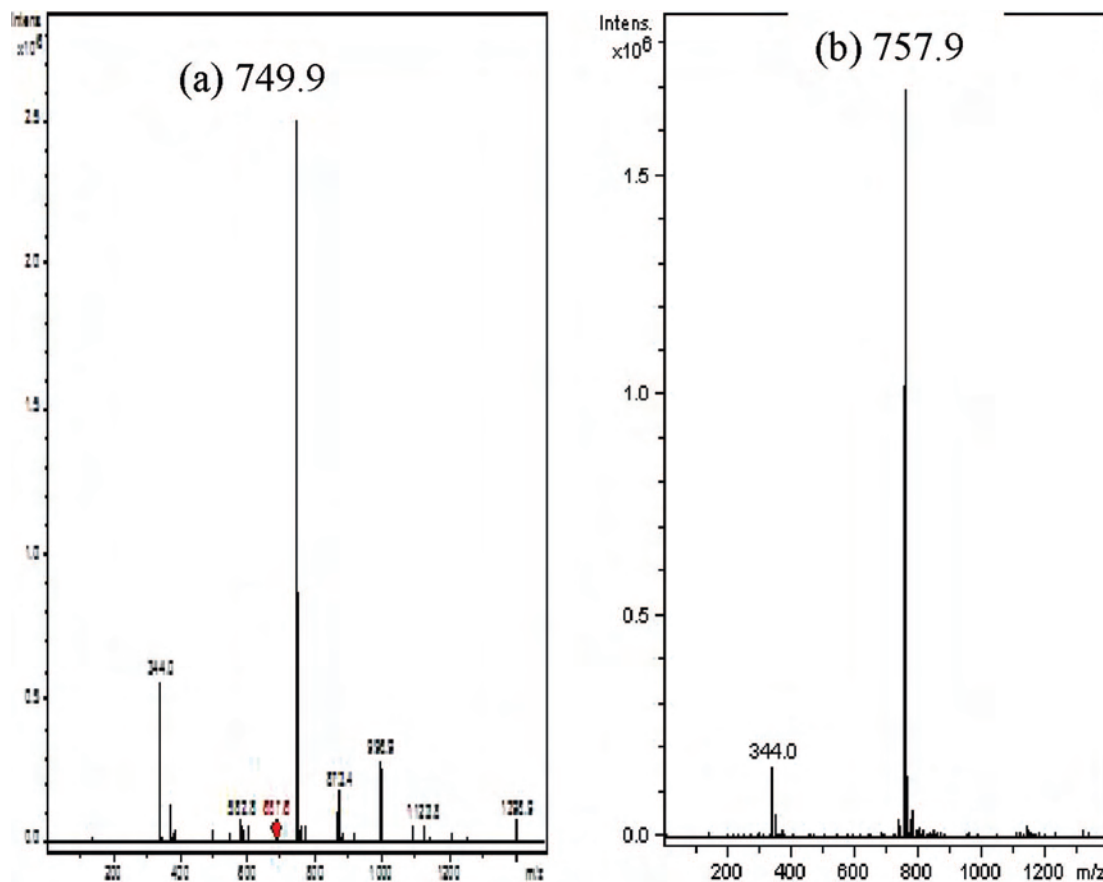


Figure 3. MS spectra of (a) $[\text{Pt}^{\text{IV}}(\text{NH}_3)_2(\text{cGMP})(\text{Cl})(\text{CBDCA-O,O}')] (m/z\ 749.9)$ and (b) $[\text{Pt}^{\text{IV}}(\text{dach})(\text{cGMP})\text{Cl}_3] (m/z\ 757.9)$ from the reaction of $\text{Pt}^{\text{IV}}(\text{dach})\text{Cl}_4/[\text{Pt}^{\text{II}}(\text{NH}_3)_2(\text{CBDCA-O,O}')]/\text{cGMP}$ (5/2/20 mM).

$[\text{Pt}^{\text{IV}}(\text{dach})(^{37}\text{Cl})_2(^{35}\text{Cl})_2]$ followed by the addition of 9-EtG, generating *trans,cis*- $[\text{Pt}^{\text{IV}}(\text{dach})(9\text{-EtG})(^{37}\text{Cl})(^{35}\text{Cl})_2]$. The $[\text{Pt}^{\text{II}}(\text{dach})(^{37}\text{Cl})_2]$ product could not be detected by LC/MS. However, $[\text{Pt}^{\text{II}}(\text{dach})(^{37}\text{Cl})(9\text{-EtG})]$ was detected at $m/z\ 524.0$ (Supporting Information), which is an indirect evidence of the generation of $[\text{Pt}^{\text{II}}(\text{dach})(^{37}\text{Cl})_2]$.

Determination of the Kinetic Rate Law for the Substitution. Figure 5a compares the time course of A_{390} of $[\text{Pt}^{\text{IV}}(\text{dach})\text{Cl}_4]/\text{cGMP}/[\text{Pt}^{\text{II}}(\text{dach})\text{Cl}_2]$ at varied concentrations of each component. The kinetic curves for different concentrations were obtained four times, and the average A_{390} versus time is displayed in Figure 5b. As seen in Figure 5b and Table 1, within experimental error, the initial rate was reduced by half when the concentration of one component was reduced by half. Therefore, the substitution reaction follows the third-order rate law with first-order for each $[\text{Pt}^{\text{IV}}]$, G, and $[\text{Pt}^{\text{II}}]$. Our result is consistent with the known rate law for the BP Pt^{II} -catalyzed Pt^{IV} -substitution reaction.¹¹ The rate law and identification of the $\text{Pt}^{\text{IV}}\text{G}$ species is the sound basis of eq 1 in Scheme 1.

Reactions of 5'-dGMP with $[\text{Pt}^{\text{IV}}(\text{en})(\text{OCOCF}_3)_2\text{Cl}_2]$, $[\text{Pt}^{\text{IV}}(\text{a,cha})(\text{OCOCH}_3)_2\text{Cl}_2]$, $[\text{Pt}^{\text{IV}}(\text{en})(\text{OH})_2\text{Cl}_2]$, $[\text{Pt}^{\text{IV}}(\text{en})\text{Cl}_4]$, and $[\text{Pt}^{\text{IV}}(\text{en})\text{Br}_4]$: Effect of Axial Ligands. Figure 6 compares A_{360} versus time of the reactions of 5'-dGMP with $[\text{Pt}^{\text{IV}}(\text{en})(\text{OCOCF}_3)_2\text{Cl}_2]$, $[\text{Pt}^{\text{IV}}(\text{a,cha})(\text{OCOCH}_3)_2\text{Cl}_2]$, $[\text{Pt}^{\text{IV}}(\text{en})(\text{OH})_2\text{Cl}_2]$, $[\text{Pt}^{\text{IV}}(\text{en})\text{Cl}_4]$, and $[\text{Pt}^{\text{IV}}(\text{en})\text{Br}_4]$. The A_{360} of $[\text{Pt}^{\text{IV}}(\text{en})(\text{OCOCF}_3)_2\text{Cl}_2]$, $[\text{Pt}^{\text{IV}}(\text{a,cha})(\text{OCOCH}_3)_2\text{Cl}_2]$, and $[\text{Pt}^{\text{IV}}(\text{en})(\text{OH})_2\text{Cl}_2]$ does not change over time, indicating that

these complexes did not react. The decrease of A_{360} of $[\text{Pt}^{\text{IV}}(\text{en})\text{Cl}_4]$ and $[\text{Pt}^{\text{IV}}(\text{en})\text{Br}_4]$ reactions indicates that both of these Pt^{IV} complexes oxidized 5'-dGMP. This was confirmed by detection of 8-oxo-5'-dGMP in the reaction mixture by HPLC and LC/MS.

The rate constants for the reactions of $[\text{Pt}^{\text{IV}}(\text{en})\text{Cl}_4]$ and $[\text{Pt}^{\text{IV}}(\text{en})\text{Br}_4]$ with 5'-dGMP at pH 6.5 and 30 °C were obtained by fitting A_{360} versus time data to eqs 1 and 2 in Scheme 1 using *DynaFit*.¹³ As shown above, the rate law for the first reaction in Scheme 1 (eq 1) follows the third-order rate law with first-order in $[\text{Pt}^{\text{II}}]$, $[\text{Pt}^{\text{IV}}]$, and G (entering group). The close agreement between experimental and modeled absorbance versus time is shown in Figure 6b,c. The k_s values are 28.5 and 1360 $\text{M}^{-2}\ \text{s}^{-1}$ for $[\text{Pt}^{\text{IV}}(\text{en})\text{Cl}_4]$ and $[\text{Pt}^{\text{IV}}(\text{en})\text{Br}_4]$, respectively. The k_e values are 1.4×10^{-4} and $0.4 \times 10^{-4}\ \text{s}^{-1}$ for $[\text{Pt}^{\text{IV}}(\text{en})\text{Cl}_4]$ and $[\text{Pt}^{\text{IV}}(\text{en})\text{Br}_4]$, respectively. The values are shown in Table 2.

Reactions of 5'-dGMP with $[\text{Pt}^{\text{IV}}(\text{NH}_3)_2\text{Cl}_4]$, $[\text{Pt}^{\text{IV}}(\text{en})\text{Cl}_4]$, and $[\text{Pt}^{\text{IV}}(\text{dach})\text{Cl}_4]$: Effect of Carrier Ligands. The reactions of 5'-dGMP with $[\text{Pt}^{\text{IV}}(\text{NH}_3)_2\text{Cl}_4]$, $[\text{Pt}^{\text{IV}}(\text{en})\text{Cl}_4]$, and $[\text{Pt}^{\text{IV}}(\text{dach})\text{Cl}_4]$ at 50 °C are compared in Figure 7. The kinetic rate constants were obtained by fitting A_{360} versus time data to eqs 1 and 2 in Scheme 1 using *DynaFit*.¹³ The close agreement between the experimental and modeled A_{360} versus time is shown in Figure 6. The k_s values are 85.8, 25.2, and 11.1 $\text{M}^{-2}\ \text{s}^{-1}$ for $[\text{Pt}^{\text{IV}}(\text{NH}_3)_2\text{Cl}_4]$, $[\text{Pt}^{\text{IV}}(\text{en})\text{Cl}_4]$, and

(13) Kuzmic, P. *Anal. Biochem.* **1996**, *237*, 260–273.

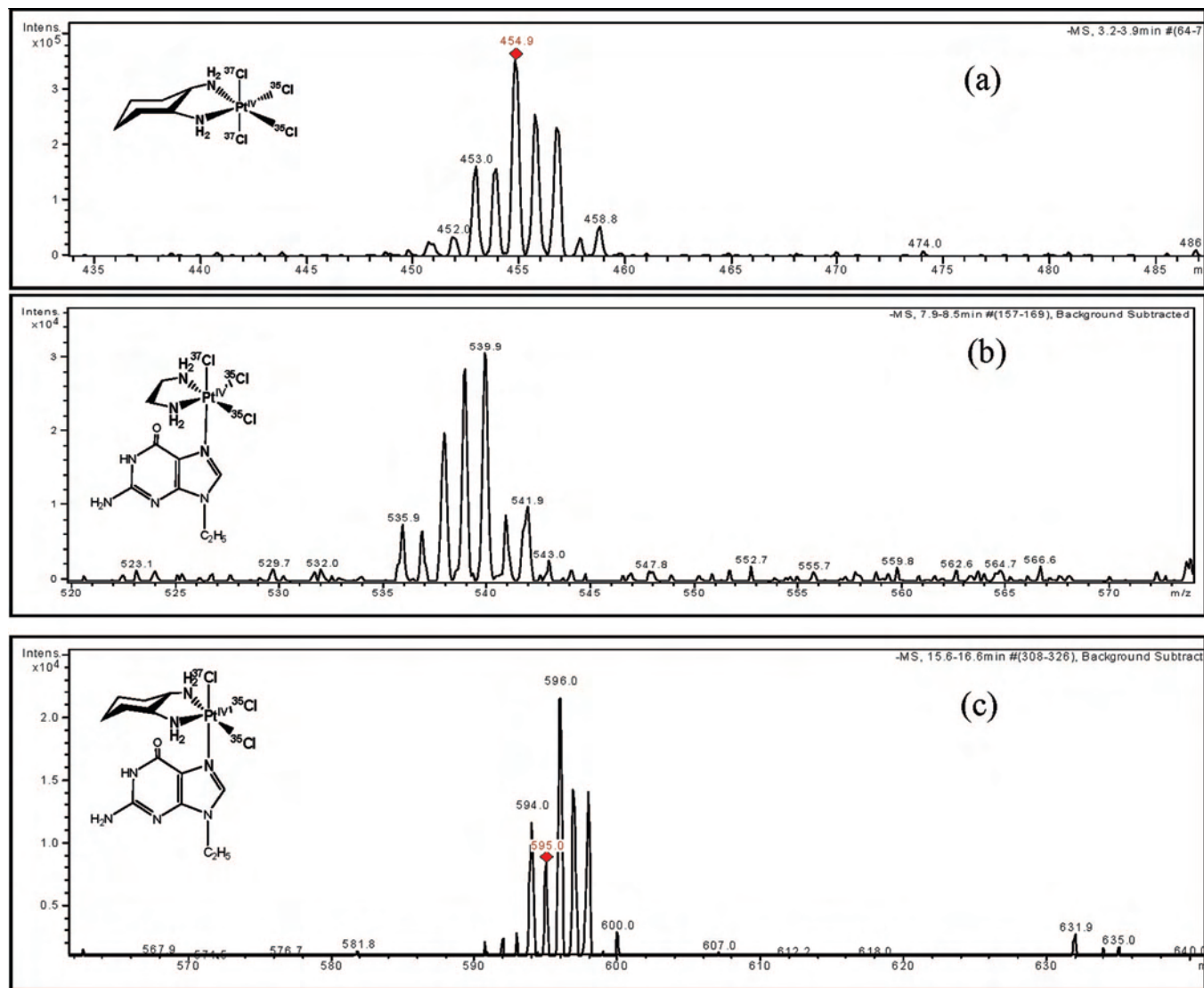


Figure 4. MS spectra of (a) $[\text{Pt}^{\text{IV}}(\text{dach})^{37}\text{Cl}_2^{35}\text{Cl}_2]$, (b) $[\text{Pt}^{\text{IV}}(\text{en})(9\text{-EtG})(^{37}\text{Cl})(^{35}\text{Cl})_2]$, and (c) $[\text{Pt}^{\text{IV}}(\text{dach})(9\text{-EtG})(^{37}\text{Cl})(^{35}\text{Cl})_2]$ from the reaction of $[\text{Pt}^{\text{II}}(\text{en})^{35}\text{Cl}_2]/[\text{Pt}^{\text{IV}}(\text{dach})(^{37}\text{Cl})_2(^{35}\text{Cl})_2]/9\text{-EtG}$ (0.5/1/1.5 mM) at 50 °C.

$[\text{Pt}^{\text{IV}}(\text{dach})\text{Cl}_4]$, respectively. The k_e values are 1.5×10^{-4} , 1.5×10^{-4} , and $14.2 \times 10^{-4} \text{ s}^{-1}$ for $[\text{Pt}^{\text{IV}}(\text{NH}_3)_2\text{Cl}_4]$, $[\text{Pt}^{\text{IV}}(\text{en})\text{Cl}_4]$, and $[\text{Pt}^{\text{IV}}(\text{dach})\text{Cl}_4]$, respectively. The values are summarized in Table 3.

Discussion

As shown in Figures 1 and 2, $[\text{Pt}^{\text{II}}(\text{NH}_3)_2(\text{CBDCA-O,O}')]_2$ accelerates the reaction of $[\text{Pt}^{\text{IV}}(\text{dach})\text{Cl}_4]$ with 5'-dGMP and with cGMP. The former is a redox reaction that involves a substitution followed by an electron transfer between Pt^{IV} and 5'-dGMP, and the latter is only a substitution reaction. Therefore, it can be deduced that $[\text{Pt}^{\text{II}}(\text{NH}_3)_2(\text{CBDCA-O,O}')]_2$ accelerates the substitution step in the redox reaction. This type of substitution mechanism is consistent with the BP mechanism (Scheme 2).¹¹ The scheme is fundamentally the BP scheme¹¹ adapted to our system. The first step is a binding of the G derivative to $[\text{Pt}^{\text{II}}\text{A}_2\text{B}_2]$ at the fifth position to produce a five-coordinate $[\text{Pt}^{\text{II}}\text{A}_2\text{B}_2\text{G}]$. Like other researchers in the literature, we could not detect this five-coordinate species. However, it is generally accepted as a

short-lived intermediate for the Pt^{II} -substitution¹⁴ and the Pt^{II} -catalyzed Pt^{IV} -substitution mechanism.¹¹ In the square-planar Pt^{II} -substitution reaction, the geometry of the five-coordinate species is thought to be trigonal-bipyramidal because it is able to account for all of the experimental evidence available.¹⁴ In the Pt^{II} -catalyzed Pt^{IV} -substitution reaction, the geometry of the five-coordinate species was not explicitly discussed in the literature. However, because of the retention of the geometric configuration for the *trans* Pt^{IV} substrate in all of the reactions studied, the five-coordinate species is drawn as square-pyramidal in our scheme.

The five-coordinate $[\text{Pt}^{\text{II}}\text{A}_2\text{B}_2\text{G}]$ subsequently binds to $[\text{Pt}^{\text{IV}}\text{C}_2\text{X}_2\text{D}_2]$ through a halo bridge to form a dimer. This dimer could not be detected, perhaps because it is a short-lived intermediate. In the dimer, two electrons transfer from the Pt^{II} center to the Pt^{IV} center, generating the new species $[\text{Pt}^{\text{IV}}\text{A}_2\text{XGB}_2]$ and $[\text{Pt}^{\text{II}}\text{C}_2\text{D}_2]$. The new $[\text{Pt}^{\text{II}}\text{C}_2\text{D}_2]$ complex was detected as $[\text{Pt}^{\text{II}}(\text{dach})\text{Cl}_2]$ from the $[\text{Pt}^{\text{IV}}(\text{dach})\text{Cl}_4]/$

(14) Langford, C. H.; Gray, H. B. *Ligand Substitution Processes*; W. A. Benjamin Inc.: New York, 1965; pp 18–48.

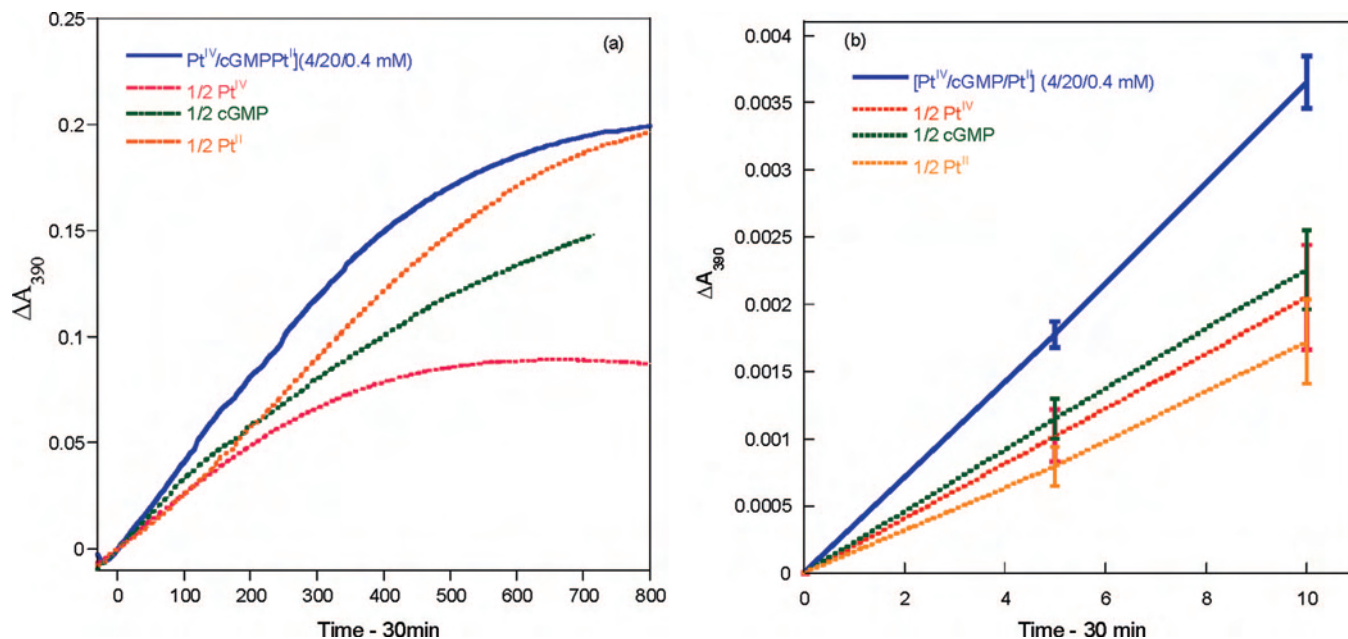
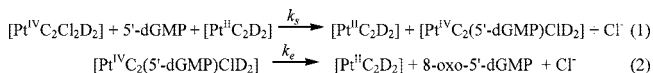


Figure 5. (a) A_{390} vs time of the reactions of $[\text{Pt}^{\text{IV}}(\text{dach})\text{Cl}_4]$, cGMP, and $[\text{Pt}^{\text{II}}(\text{dach})\text{Cl}_2]$ in 100 mM NaCl at 20 °C and pH 8.2. Because of the spectral noise during the first 30 min initial period, 30 min was subtracted from the time scale. The absorbance was made zero at 30 min in order to show the first 10 min (actually 30–40 min after starting the reaction) absorbance difference clearly. (b) Average A_{390} from the four sets of reactions with the same concentration of each component.

Table 1. Initial Rates for the Reaction of $[\text{Pt}^{\text{IV}}(\text{dach})\text{Cl}_4]/\text{cGMP}/[\text{Pt}^{\text{II}}(\text{dach})\text{Cl}_2]$ at Different Concentrations at 25 °C

$[\text{Pt}^{\text{IV}}(\text{dach})\text{Cl}_4]/\text{cGMP}/$ $[\text{Pt}^{\text{II}}(\text{dach})\text{Cl}_2]$ mM	rate 1 $\times 10^4 \text{ M}^{-1} \text{ s}^{-1}$	rate 2 $\times 10^4 \text{ M}^{-1} \text{ s}^{-1}$	rate 3 $\times 10^4 \text{ M}^{-1} \text{ s}^{-1}$	rate 4 $\times 10^4 \text{ M}^{-1} \text{ s}^{-1}$	average rate $\times 10^4 \text{ M}^{-1} \text{ s}^{-1}$
4/20/0.4	3.7	3.4	3.6	3.9	3.7 ± 0.2
2/20/0.4	2.6	2.0	2.1	1.6	2.1 ± 0.4
4/10/0.4	2.6	2.1	1.9	2.5	2.3 ± 0.3
4/20/0.2	2.2	1.4	1.8	1.5	1.7 ± 0.3

Scheme 1. Kinetic Model for the Oxidation of 5'-dGMP by $[\text{Pt}^{\text{IV}}\text{C}_2\text{Cl}_2\text{D}_2]$



5'-dGMP reaction previously by IR⁸ and ¹H NMR.^{7–9} It again reacts with G followed by $[\text{Pt}^{\text{IV}}\text{C}_2\text{X}_2\text{D}_2]$, generating $[\text{Pt}^{\text{IV}}\text{C}_2\text{GXD}_2]$ and $[\text{Pt}^{\text{II}}\text{C}_2\text{D}_2]$. The LC/MS detection of $[\text{Pt}^{\text{IV}}(\text{en})(5'\text{-dGMP})\text{Cl}_3]$ and $[\text{Pt}^{\text{IV}}(\text{dach})(5'\text{-dGMP})\text{Cl}_3]$ from the $[\text{Pt}^{\text{IV}}(\text{dach})\text{Cl}_4]/[\text{Pt}^{\text{II}}(\text{en})\text{Cl}_4]/5'\text{-dGMP}$ reaction¹⁰ and $[\text{Pt}^{\text{IV}}(\text{NH}_3)_2(\text{cGMP})(\text{Cl})(\text{CBDCA-O,O})]$ and $[\text{Pt}^{\text{IV}}(\text{dach})(\text{cGMP})\text{-Cl}_3]$ (Figure 3b,c) from the $[\text{Pt}^{\text{IV}}(\text{dach})\text{Cl}_4]/[\text{Pt}^{\text{II}}(\text{NH}_3)_2(\text{CBDCA-O,O})]/\text{cGMP}$ reaction mixture is consistent with the BP mechanism.

The detection of *trans,cis*- $[\text{Pt}^{\text{IV}}(\text{en})(9\text{-EtG})(^{37}\text{Cl})(^{35}\text{Cl})_2]$ and *trans,cis*- $[\text{Pt}^{\text{IV}}(\text{dach})(9\text{-EtG})(^{37}\text{Cl})(^{35}\text{Cl})_2]$ (Figure 4) from the $[\text{Pt}^{\text{II}}(\text{en})(^{35}\text{Cl})_2]/\text{trans,cis}-[\text{Pt}^{\text{IV}}(\text{dach})(^{37}\text{Cl})(^{35}\text{Cl})_2]/9\text{-EtG}$ reaction mixture is also consistent with Scheme 2. The substitution can be thought of as an oxidative addition reaction of the planar Pt^{II} complex in which the entering ligand G and the halo ligand from the Pt^{IV} complex are added to the Pt^{II} complex in the axial positions. From the original Pt^{IV} point of view, the axial halo ligand is substituted by the G derivative.

The Pt^{IV} complexes such as *trans,cis*- $[\text{Pt}^{\text{IV}}(\text{en})(\text{OH})_2\text{Cl}_2]$, *trans,cis*- $[\text{Pt}^{\text{IV}}(\text{en})(\text{OCOCF}_3)_2\text{Cl}_2]$, and *cis,trans,cis*- $[\text{Pt}^{\text{IV}}(\text{NH}_3)(\text{C}_6\text{H}_{11}\text{NH}_2)(\text{OCOCH}_3)_2\text{Cl}_2]$ do not oxidize 5'-dGMP (Figure

6). The required substitution for the redox reaction could not occur because OH, OCOCF_3 , and OCOCH_3 are not suitable bridging ligands for the inner-sphere electron transfer. Their lowest empty orbitals for the electron transfer are at a relatively high energy.¹¹ On the other hand, chloro and bromo complexes readily react, particularly the bromo complex. As shown in Figures 6b,c, the reaction completion time of 1 mM $[\text{Pt}^{\text{IV}}(\text{en})\text{Cl}_4]$ is about 70 h while that of 0.3 mM $[\text{Pt}^{\text{IV}}(\text{en})\text{Br}_4]$ is about 7 h under the same reaction conditions. This is due to the 50-fold larger substitution rate (k_s) of the bromo complex in spite of the slower electron-transfer rate (k_e) compared to the chloro complex. The heavier and more polarizable bromo ligand has lower-energy orbitals available that can participate in bridge formation and thus provide an effective path for the electron transfer from the Pt^{II} to Pt^{IV} centers.¹¹

It is also interesting to note that the reactivities of these complexes with 5'-dGMP and with ascorbate are significantly different. The redox rates for reaction with ascorbate are dependent on the magnitude of the reduction potentials of the Pt^{IV} complexes, which are in the order *trans,cis*- $[\text{Pt}^{\text{IV}}(\text{en})(\text{OH})_2\text{Cl}_2] < \text{cis,trans,cis}-[\text{Pt}^{\text{IV}}(\text{NH}_3)(\text{C}_6\text{H}_{11}\text{NH}_2)(\text{OCOCH}_3)_2\text{Cl}_2] < [\text{Pt}^{\text{IV}}(\text{en})\text{Cl}_4] < \text{trans,cis}-[\text{Pt}^{\text{IV}}(\text{en})(\text{OCOCF}_3)_2\text{Cl}_2]$.⁶ The $[\text{Pt}^{\text{IV}}(\text{en})(\text{OCOCF}_3)_2\text{Cl}_2]$ complex, which is quickly reduced by ascorbate, does not react with 5'-dGMP. Apparently, Pt^{IV} reacts with ascorbate via a mechanism different

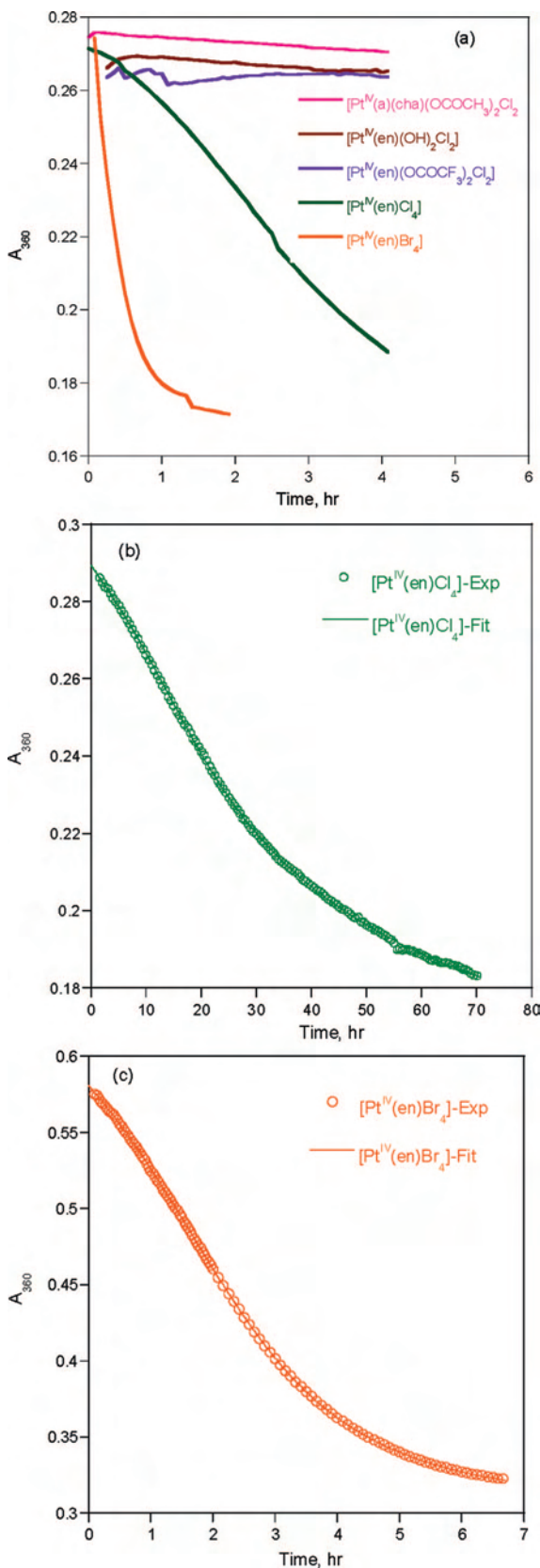


Figure 6. Absorbance at 360 nm vs time of Pt^{IV} complexes with 5'-dGMP. Reaction conditions: (a) [Pt^{IV}(en)(OH)₂Cl₂]/[Pt^{II}(en)Cl₂]/5'-dGMP/NaCl (2/0.2/50/100 mM), [Pt^{IV}(en)(OCOCF₃)₂]/[Pt^{II}(en)Cl₂]/5'-dGMP/NaCl (2/0.2/50/100 mM), [Pt^{IV}(a,cha)(OCOCH₃)₂Cl₂]/5'-dGMP/NaCl (2/50/100 mM), [Pt^{IV}(en)Cl₄]/[Pt^{II}(en)Cl₂]/5'-dGMP/NaCl (2/0.2/50/100 mM), [Pt^{IV}(en)Br₄]/5'-dGMP/KBr (0.3/50/100 mM), pH 6.5 at 30 °C. (b) [Pt^{IV}(en)Cl₄]/5'-dGMP/NaCl (1/5/100 mM), pH 6.5 at 30 °C. (c) [Pt^{IV}(en)Br₄]/5'-dGMP/KBr (0.3/5/100 mM), pH 6.5 at 30 °C.

Table 2. Substitution and Electron-Transfer Rates for the Reaction of Pt^{IV} Complexes with 5'-dGMP^a

	[Pt ^{IV} (en)Cl ₄]	[Pt ^{IV} (en)Br ₄]	[Pt ^{IV} (dach)Cl ₄]
k_s (M ⁻² s ⁻¹)	28.5 ± 1.6	1360 ± 50	8.1 ± 2.7
$k_e \times 10^4$ (s ⁻¹)	1.4 ± 0.5	0.4 ± 0.2	3.2 ± 0.8

^a The rate constants were obtained from the kinetic curves in Figure 5b,c for reactions [Pt^{IV}(en)Cl₄]/5'-dGMP/NaCl (1/5/100 mM) and [Pt^{IV}(en)Br₄]/5'-dGMP/KBr (0.3/5/100 mM), pH 6.5 at 30 °C. Values are reported as ±1 standard deviation of the mean for three measurements.

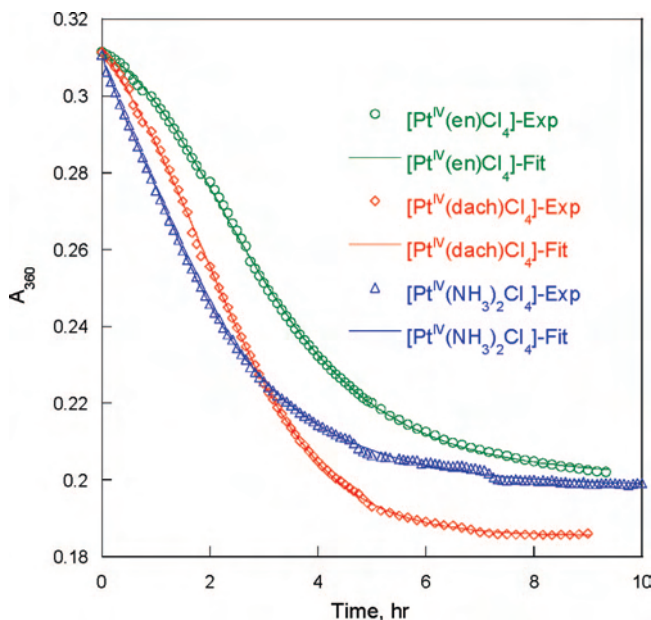


Figure 7. Absorbance at 360 nm vs time of [Pt^{IV}(en)Cl₄]/[Pt^{II}(en)Cl₂]/5'-dGMP (1/0.2/20 mM), [Pt^{IV}(dach)Cl₄]/[Pt^{II}(dach)Cl₂]/5'-dGMP (1/0.2/20 mM), [Pt^{IV}(NH₃)₂Cl₄]/[Pt^{II}(NH₃)₂Cl₂]/5'-dGMP (1/0.2/20 mM) reactions in 100 mM NaCl, pH 8.3 at 50 °C.

Table 3. Substitution and Electron-Transfer Rates for the Reaction of Pt^{IV} Complexes with 5'-dGMP^a

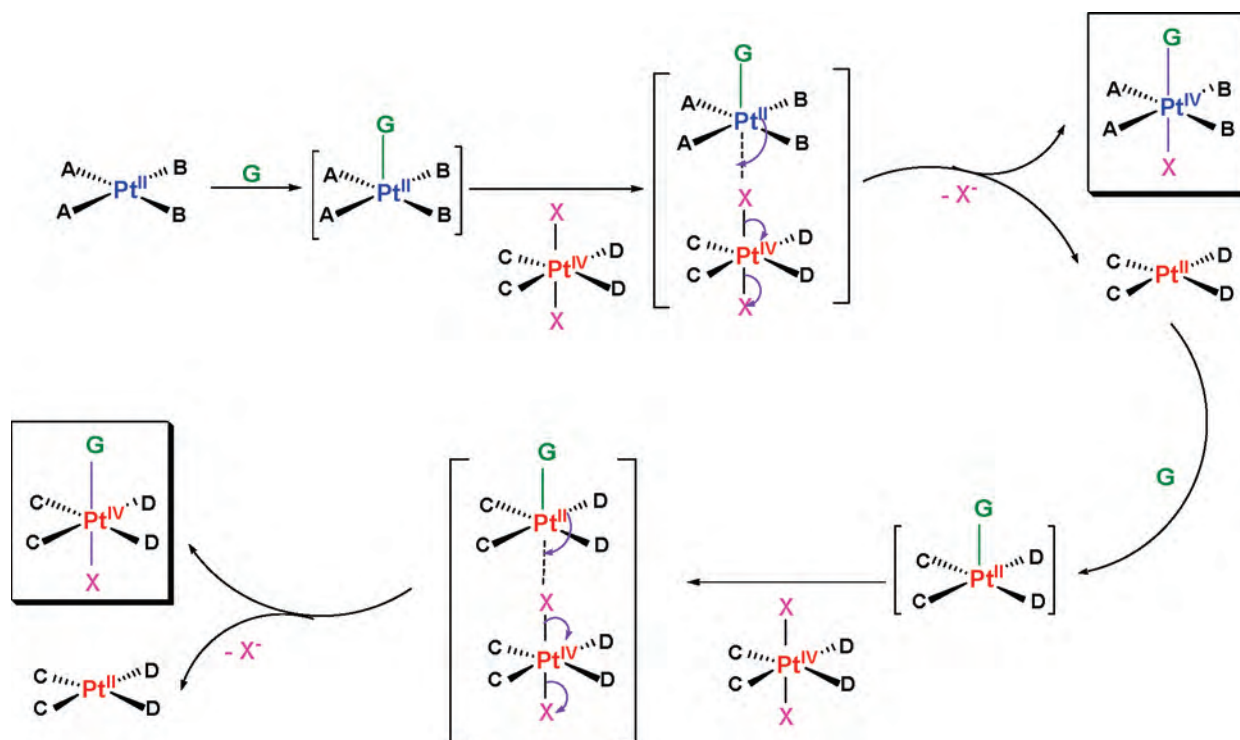
	[Pt ^{IV} (NH ₃) ₂ Cl ₄]	[Pt ^{IV} (en)Cl ₄]	[Pt ^{IV} (dach)Cl ₄]
k_s (M ⁻² s ⁻¹)	85.8 ± 6.2	25.2 ± 4.1	11.1 ± 2.2
$k_e \times 10^4$ (s ⁻¹)	1.5 ± 0.1	1.5 ± 0.1	14.2 ± 0.8

^a The rate constants were obtained from the kinetic curves in Figure 6 for the reactions of [Pt^{IV}(en)Cl₄]/[Pt^{II}(en)Cl₂]/5'-dGMP (1/0.2/20 mM), [Pt^{IV}(dach)Cl₄]/[Pt^{II}(dach)Cl₂]/5'-dGMP (1/0.2/20 mM), and [Pt^{IV}(NH₃)₂Cl₄]/[Pt^{II}(NH₃)₂Cl₂]/5'-dGMP (1/0.2/20 mM) reactions in 100 mM NaCl, pH 8.3 at 50 °C. Values are reported as ±1 standard deviation of the mean for three measurements.

from that with 5'-dGMP. Depending on the structure of Pt^{IV}, reductive elimination,¹⁵ and outer- and inner-sphere¹⁶ mechanisms have been proposed for reduction by ascorbate.

When Pt^{IV} complexes with different carrier ligands but the same chloro axial ligands are compared, the k_s values increase in the order [Pt^{IV}(dach)Cl₄] < [Pt^{IV}(en)Cl₄] < *cis*-[Pt^{IV}(NH₃)₂Cl₄], which is the inverse order of their carrier ligand size. The smaller the carrier ligand, the less steric hindrance for the bridge formation. The values for the rate constant, k_e for [Pt^{IV}(NH₃)₂Cl₄] and *cis*-[Pt^{IV}(en)Cl₄] are

- (15) (a) Lemma, K.; Shi, T.; Elding, L. I. *Inorg. Chem.* **2000**, *39*, 1728–1734. (b) Lemma, K.; Sargeson, A. M.; Elding, L. I. *J. Chem. Soc., Dalton Trans.* **2000**, 1167–1172. (c) Lemma, K.; Berglund, J.; Farrell, N.; Elding, L. I. *J. Biol. Inorg. Chem.* **2000**, *5*, 300–306.
- (16) (a) Evans, D. J.; Green, M. *Inorg. Chim. Acta* **1987**, *130*, 183–184. (b) Bose, R. N.; Weaver, E. L. *J. Chem. Soc., Dalton Trans.* **1997**, 1797–1799. (c) Hindmarsh, K.; House, D. A.; van Eldik, R. *Inorg. Chim. Acta* **1998**, *278*, 32–42. (d) Weaver, E. L.; Bose, R. N. *J. Inorg. Biochem.* **2003**, *95*, 231–239.

Scheme 2. Proposed Mechanism for the Pt^{II}-Accelerated Pt^{IV}-Substitution Reaction for Guanosine Derivatives

The scheme is fundamentally the BP scheme¹¹ adapted to our system. The intermediates were not detected experimentally and are marked in brackets. Because both [Pt^{IV}A₂GXB₂] and [Pt^{IV}C₂GXD₂] can generate 8-oxo-5'-dGMP, when G is 5'-dGMP, the Pt^{II} analogues should be Pt^{IV} complexes (A = C and B = D) when k_s and k_e of [Pt^{IV}C₂X₂D₂] are obtained.

similar, but k_s of the former is 3-fold larger, resulting in a faster rate for the overall redox reaction. The *cis*-[Pt^{IV}(NH₃)₂Cl₄] complex has a 7-fold higher k_s but a 10-fold lower k_e than [Pt^{IV}(dach)Cl₄], resulting in the faster overall redox rate during the first half of the reaction time (Figure 7). Taken together, these results strongly suggest that substitution plays a critical role in the overall redox reaction between 5'-dGMP and Pt^{IV} and is consistent with the BP mechanism.

Conclusion

We have shown that the substitution step is essential for the oxidation of 5'-dGMP by Pt^{IV}. The substitution is accelerated by Pt^{II} and follows the BP mechanism. The Pt^{II} complex does not have to possess a halo leaving group and, therefore, the substitution can be thought of as an oxidative addition reaction of the planar Pt^{II} complex in which the entering ligand G and the halo ligand from the Pt^{IV} complex are added to the Pt^{II} complex in the axial positions. From

the original Pt^{IV} point of view, the axial halo ligand is substituted by the G derivative. The Pt^{IV} complex must possess axial halo ligands for the substitution, and those with a larger axial halo and a smaller carrier ligand exhibit higher substitution rates.

Acknowledgment. This work was supported by the National Science Foundation (Grants CHE-0450060 and CHE-0707357). Financial support is acknowledged from the NSF (Grant CHE-0520708) for their support in the purchase of the LC/MS system used in the course of this work. We are grateful to Drs. K. Wosikowski and C. Probst at GPC Biotech AG for satraplatin.

Supporting Information Available: MS spectrum of [Pt^{II}(dach)-(³⁷Cl)(9-EtG)]. This material is available free of charge via the Internet at <http://pubs.acs.org>.

IC701868B